IOŚ-PIB Environmental Protection and Natural Resources
Ochrona Środowiska i Zasobów Naturalnych
sciendo Vol. 35 No 3(101): 1-20
DOI 10.2478/oszn-2025-0005

Krzysztof Muszyński*

Modelling of rainwater reduction and hydrological performance of selected green infrastructure (GI) facilities in urban catchments

* Cracow University of Technology, Cracow, Poland
e-mail: krzysztof.muszynski@pk.edu.pl

Keywords:
rainwater runoff, stormwater management, green infrastructure, runoff reduction, peak flow reduction, GI performance, SWMM LID modelling, SWMM single-event calibration; rain garden performance

Abstract

Currently, effective rainwater management in urban areas requires a modern and comprehensive approach, with mathematical modelling methods at its foundation. The aim of this study was to estimate the impact of the use of dispersed green infrastructure (GI) – specifically, drainage-equipped rain gardens (bio-retention cells, or BC) – and their operational hydrological performance on the scale of an urban catchment, particularly in reducing the amount of rainwater discharged directly to the receiver. An additional objective was to determine the relationship between the total rainwater inflow per unit area and the capacity percentage reduction in individual BC facilities. In this research, a hydrodynamic single-event precipitation model was built and calibrated for an existing housing estate in Cracow (Poland) using the Storm Water Management Model (SWMM). The functioning of the GI is represented by Low Impact Development (LID), which was simulated for a number of precipitation scenarios (S_0–S_7) with durations of 4.2, 15, 30, 45, 60, 90, 120 and 180 minutes, and a probability of occurrence of p = 10% (indicating a 10% chance of occurrence in any given year).

The results demonstrated significant potential for reducing the peak flow of rainwater by an average of 94%, and reducing the total volume of rainwater by an average of 86%, for all simulated precipitation at the outfall of the entire system. Analysis of individual BC facilities revealed reductions in rainwater ranging from 67% to 95% of capacity for GI facilities, depending on the duration of the rainfall. Notably, more significant reductions in GI facilities were observed in cases of short, intense rainfall. The analysis of the individual BC facilities with the highest efficiency showed that the maximum values of total inflow per 1 m^2 of their surface area, reduced to 100% for rainwater inflow, occurred during heavy rainfall of 15 min (S_1) and amounted to 29.72 L/m^2 (average 5.79 L/m^2).

1. INTRODUCTION

According to a memorandum by the United States Environmental Protection Agency (USEPA) [Grumbles 2007], green infrastructure (GI) refers to objects that mimic natural processes of infiltration and evapotranspiration while enabling the proper recharge of groundwater and maintaining appropriate flow, as well as hydrological and hydraulic stability. Global warming and ongoing climate change increase the risk of flooding [Muller 2007], increasing the need for proper rainwater management. However, this is a major logistical and technical challenge, especially in urban areas, where the existing and often dense development makes it difficult or completely impossible to use GI.

Rainwater drainage systems effectively manage water runoff in urbanized areas; however, under certain conditions, such as heavy rainfall, they are the infrastructural component that contributes most to hazards, such as flash floods. Such phenomena have been successfully modelled using the Storm Water Management Model (SWMM) engine [Nur Oktalinov Fikri et al. 2022], which helps understand the impact of the increase in rainfall frequency on the formation of hazards and in the process improving the operation of drainage systems. It is important that spatial databases be integrated with hydrological and meteorological information, as this enables the identification of relationships between individual processes both directly and indirectly linked to flash flooding [Tarek et al. 2017]. One of the options for mitigating the effects of flooding in urban spaces is retention reservoirs, which may be used even in such difficult places as airport areas [Barszcz 2017]. The location of these retention reservoirs may also be optimized in an urban rainwater drainage system [Wang et al. 2017]. SWMM modelling is used for detailed analysis of the structure of such networked reservoirs in terms of minimizing and preventing overloading of rainwater collectors [Dąbrowski et al. 2022]. This is influenced by the

Open Access. © Author(s), published by Sciendo. BY-NC-ND This is an open access article licensed under the Creative Commons Attribution-NonCommercial-NoDerivs License (http://creativecommons.org/licenses/by-nc-nd/3.0/).

location of the rainwater supply and drainage channels, among other factors.

Drainage-equipped rain gardens, also known as bio-retention cells (BC), are relatively simple in their design and operation, and their functionality has been researched in a variety of applications, including planning methods and urban agriculture; assessment approaches; sustainability and climate adaptation; and ecosystem services and their benefits [Korkou et al. 2023]. The well-documented positive outcomes of these uses [Choi et al. 2021] stem from employing natural processes to mitigate the impacts of climate change and supporting other socially sustainable development goals, including both quantitative and qualitative protection of receiving waters; runoff reduction; minimization of flooding; the prevention of groundwater pollution in urban ecosystems; increased biodiversity; and improving microclimate control [Kasprzyk et al. 2022] by lowering air temperatures and increasing ambient humidity. It has also been observed [Wang et al. 2018] that the quality and quantity of peak surface runoff are more significantly influenced by urbanization factors (especially by land-use intensity and population density) than by those related to climate change. Therefore, the implementation of GI and the reduction of impervious surface areas should be given serious consideration in both existing and newly-developed urban areas.

GI has been modelled in the SWMM software by researchers and engineers worldwide, creating an example of Low Impact Development (LID). GI is recognized as a popular tool for reducing the quantity and improving the quality of surface runoff from impervious surfaces [Roy et al. 2014], [Huang et al. 2020]. It has an important role in addressing problems that have arisen from the interaction between urbanization, climate change, and demography.

It is well known that, due to impervious surfaces' concomitant limitation of biologically active areas, surface runoff is increased and accelerated [Li et al. 2018], [Zhang et al. 2018], and stormwater pollutant concentrations are increased [Wang et al. 2013], [Das et al. 2018], [Godyń et al. 2023]. GI has been demonstrated [Rahman et al. 2020] to increase transpiration and reduce ambient temperatures, contributing to the minimization of urban heat islands while effectively reducing pollutants such as total suspended solids [Tiveron et al. 2018]. Godyń et al. [2024] estimated the impact of GI at the urban-catchment scale and assessed its ability to mitigate environmental risks. Another research project evaluated the benefits and effectiveness of 165 rain barrels and 81 rain gardens installed on 30% of properties in four experimental catchments [Roy et al. 2014]. Measures taken to mimic natural ecosystems have been proven to have a variety of ecosystem benefits.

The runoff of rainwater from green roofs and bio-retention cells was successfully modelled using SWMM [Jeffers et al. 2022], demonstrating the accuracy of applying SWMM LID for such calculations (NSE > 0.81) while considering reasonable assumptions for individual parameters. Hamouz et al. [2020] found that the implementation of a green roof on just 11% of a roof's area can significantly reduce maximum runoff. McCutcheon et al. [2013] modelled GI using SWMM for both long-term simulations and single precipitation events and found that it generates reasonable and relevant results. On the other hand, modelling the hydrological response of green roofs requires the adaptation of many parameters, and the results of the simulations have not always been satisfactory [Burszta-Adamiak et al. 2013]. For most of the tested precipitation events, the model had limited capabilities in accurately simulating the hydrograph of rainwater runoff from green roofs, with Nash coefficients showing negative values. Therefore, the quality of green roof simulation results remains unproven.

Rezaei et al. [2019] performed an impact assessment using SWMM for vegetated swales and rain gardens to measure quantitative runoff reduction and the improvement of surface runoff quality, using field data and synthetic rainfall at high intensities of 70–90 mm. Their results showed that the peak runoff reduction decreased as rainfall intensity increased from 27% to 19%. The model was calibrated on a single actual rainfall event with an intensity of 12.5 mm; implementation of GI was followed by a peak runoff reduction of 23%.

An important study carried out in the city of Parma, Ohio analysed a 3-year period of GI operation in urban conditions [Jarden et al. 2015]. The analysis included street-connected bio-retention cells, rain gardens, and rain barrels serving about 45.7% of the residential catchment area (mainly impervious surfaces). The installation and use of GI on selected streets in a residential area of the city resulted in a peak flow reduction of approximately 33% and a total storm runoff reduction of 40%.

Reductions in peak flow and runoff volume to relieve the load on existing rainwater drainage systems can have synergistic benefits by minimizing negative impacts on receiver waters through reducing the frequency of flash floods, improving the infiltration process, increasing the recharge of groundwater aquifers [Zhang et al. 2019], and improving the habitats of regional species of flora and fauna [Granados-Olivas et al. 2016].

Actual studies of the impact of GI on receivers are not easy, but are critically needed. Urban-catchment-scale modelling is essential, and the simulation results should provide guidance for implementation of GI. A significant amount of research has been carried out on the calibration of models built with the use of continuous long-term data (e.g., [D'Ambrosio et al. 2022], [Epps et al. 2019], [Cipolla et al. 2016], and [Del Giudice et al. 2016]), as well as models based on single precipitation events (e.g., [Arjenaki et al. 2020], [Yim et al. 2016]). There were also some studies where the authors did not use a calibration process to assess model quality due to a lack of data (e.g., [Agarwal et al. 2019]) or calibrated their models using the comprehensive runoff coefficient (CRC) method [Bai et al. 2019].

The results of the research mentioned above typically focus on the percentage reduction in rainwater quantity.

Table 1. Analyzed scenarios

	Scenario S_0	Scenario S_1	Scenario S_2	Scenario S_3	Scenario S_4	Scenario S_5	Scenario S_6	Scenario S_7
Precipitation duration	90 min (4.2 mm)	15 min	30 min	45 min	60 min	90 min	120 min	180 min
Average rainfall intensity [LPS/ha]*	7.8	273.32	175.33	134.52	105.37	74.81	59.55	42.46
Total precipitation p = 10% [mm]	4.2	24.60	31.56	36.32	37.93	40.40	42.88	45.86
Precipitation intensity p = 10% [mm/hr]	2.80	98.40	63.12	48.43	37.93	26.93	21.44	15.29

* LPS – litres per second

Exceptionally, the performance of bioretention systems has been presented as the temporal behaviour of the variables such as inflow, outflow, storage capacity and infiltration in a bioretention box experiment [Batalini de Macedo et al. 2018]. These studies were carried out under laboratory conditions; the most valuable practical studies are those carried out in the field [Burszta-Adamiak et al. 2023], where, among other things, selected rainfall events were observed during which water was ponding in a rain garden. The amount of retention in the rain garden was directly influenced by the thickness of the soil layers and the infiltration process, which are described in detail by Kravchenko et al. [2024]. Field studies, laboratory experiments and mathematical modelling integrate specific indicators, and their incorporation contribute to the development of more scientific and practical systems for GI in urban environments [Mao et al. 2024].

Therefore, unit results are important because they characterise the operation of equipment under specific given conditions. Such results are difficult to generalise, but, they can be of great importance in engineering practice locally, and can serve as models for other cases with similar conditions. Considering the knowledge gaps in the field of GI efficiency and hydrological performance [Jiang et al. 2015], this study focused on the important operating parameters of BC in single-family residential buildings in the northern part of Cracow (Poland). The analysis of the existing rainwater drainage system operation, and the size and location of surface runoff routes and depression storage sites in a simulation without GI, helped identify places that are potentially more suitable for the construction of GI, along with their individual unit loads and operating parameters.

The aims of this study were to: (1) verify the possibility of implementing GI to reduce the amount of surface runoff of rainwater in an existing urbanised area; (2) show the relationship between the average reductions in total volume and peak flows for individual BC under different rainfall durations and intensities; and (3) estimate the rainwater inflow limit for an area with GI facilities under different rainfall durations and intensities at which there is a 100% quantitative reduction of inflow.

2. MATERIALS AND METHODS

A hydrodynamic model built in the SWMM environment was used to assess the impact of GI on the reduction in rainwater runoff to the receiver from the residential catchment area under study. Simulations were performed for the existing conditions using the current development conditions of the study area. The course of the rainwater drainage system was then mapped, and the rainfall and flow volumes were measured at the W_1 outfall (the location is shown in Figure 1) to the receiver on August 26, 2023.

A rainfall model created on the basis of the distribution of the phase series of rainfall maxima from 33 years (1986-2019), which is considered the most reliable tool for the dimensioning of rainwater drainage systems in Cracow, was used [Precipitation model 2024]. Calculations were performed for design rainfall with the DVWK method for the probability of occurrence of p = 10% and a duration of 15 to 180 minutes, in accordance with the recommendations of the Cracow model for dimensioning rainwater drainage systems, based on PN-EN 752:2017-06 [2017].

The prospective conditions included eight scenarios: S_0 for real precipitation, and S_1–S_7, as shown in Table 1. For scenarios S_0–S_7, selected drainage-equipped rain gardens – bio-retention cells (BC) – were integrated into the existing settlement layout.

The research approach used at the initial stage was to integrate the available databases. These were the Digital Terrain Model 1m; the Database of Topographical Objects; and the National Integration of Utilities Networks [GUGiK 2023], along with the GI Concept. The GI Concept incorporated drainage-equipped rain gardens – represented in SWMM as bio-retention cells (BC) – with the parameters for BC sourced from the literature. The quality of the input data determined all further spatial analysis

Figure 1. Location of the measuring point in the study area with catchment for the existing outfall W_1

Table 2. Spatial analyses based on the Database of Topographical Objects of the study area

Land use	Area	
	ha	%
Roofs	1.12	26.9
Roadways, pavement, alleys	0.40	9.6
Single- and multi- family residential land	2.17	52.0
Biologically active areas	0.48	11.5
TOTAL	**4.17**	**100.0**

activities, which were carried out using Geographic Information System (GIS) and Geographic Resources Analysis Support System (GRASS) software.

The results delineated the watersheds, identifying the direction and structure of the runoff flow path, the land use, and a complete and detailed rainwater drainage system. GI planning consisted of incorporating selected forms of GI into the existing urban layout of the housing estate in such a way as to maintain the entire existing development of the housing estate while changing the elevation shape as little as possible. The above analyses and data aggregation provided the foundation for creating a hydrodynamic model of the studied area in the SMWW environment. All sub-catchments were delineated and characterized in detail, including a description of their fraction of impervious area [Porębska et al. 2023].

In addition, the existing rainwater inflows to the junctions were analysed, and the drainage system supply was carefully assessed. The model, based on the precipitation and flow measurement data obtained at the W_1 outfall, was calibrated and evaluated. Finally, the model was used to run GI scenarios, and the model responses were compared and subjected to a detailed analysis.

The correctly calibrated model was fed design rainfall hyetographs for scenarios S_0–S_7. Simulations were carried out for both the existing and prospective conditions, enabling comparisons of peak flow, total flow reduction and other operating parameters of the GI facilities.

2.1. Study area

The analysed area, covering a total of 4.17 ha, is located in the northern part of the city of Cracow (Poland) and lies entirely within the hydrological catchment of the Sudół River, a right-bank tributary of the Prądnik (Białucha) River. The area is built up with housing estates of single-family residential buildings largely built around 1995 and arranged mostly in rows along a north-south axis, as shown in Figure 1. The results of spatial analyses conducted using data from the Database of Topographical Objects with the use of GIS tools are presented in Table 2.

The predominant land use class in the study area was vegetated (typically trees and shrubs on lawns between

housing blocks) with a small portion of the area comprising pedestrian and bicycle routes, as well as single-family residential land. Multi-family residential areas were a fragment of the adjacent catchment and comprised a negligible amount of the study area (0.03 ha). Grassland areas receive low runoff rates due to the significant presence of trees with broad, spreading crowns. The pedestrian and bicycle routes, separated as alleys, had mostly permeable surfaces. In addition, the roadways, including local and other roads, were made of paving blocks or hardened gravel. All the above indicates that 63.5% of the catchment area under investigation was biologically active.

According to the maps, the roofs of all existing buildings (119 units) were directly connected to the rainwater drainage system by gutter systems. The roadways, mainly covered with prefabricated paving blocks in poor condition, were equipped with inlet grates. Rainwater that does not accumulate in depression storage or manage to infiltrate joints thus predominantly enters the rainwater drainage system directly. The entire area, as shown in Figure 1, discharges into the receiver — a ditch that is a right-bank tributary of the Sudół River.

The gravity-based rainwater drainage system consists of 116 junctions, with an average depth of 2 m below ground level, and pipes totalling 1.38 km in length, with diameters of 0.15–0.5m. Outfall W_1 was measured to investigate flows during precipitation. At a distance of 350 m from the centroid of the W_1 catchment, there was a rain gauge belonging to the research network of Cracow University of Technology, Faculty of Environmental Engineering and Energy, Department of Geoengineering and Water Management.

For the purpose of determining the height and slopes of the land surface, a detailed Digital Terrain Model with a 1 m grid was used. Using this data and GIS-GRASS tools, the directions of surface runoff, subcatchments, and the slope of the land in the northern direction (towards the receiver) were determined at an average of 1.4%. The maximum elevation within the entire study area is 228.4 meters above sea level (m a.s.l.), while the minimum is 223.8 m a.s.l.

The analysis of ground conditions revealed that the soils in the study area belong to the coarse B type, characterised by above-average permeability (infiltration coefficient value: 3.8–7.6 mm·h^{-1}). The soils consist of sandy medium-deep soils, loess, and sandy loams.

With the use of aggregated data, a visualization of the imperviousness of the studied area was created. The results of the analysis are shown in Figure 2, which illustrates the studied area in terms of: (A) the layout of the entire drainage infrastructure, (B) land development, (C) altitude, location, and directions of surface water runoff determined on the basis of terrain slopes, and (D) subcatchments and imperviousness implemented in the SWMM.

2.2. Model construction and calibration

Advanced modelling requires a calibration process in order to fine-tune many input parameters that are important for the quality of the model's response [Khan et al. 2022]. In this study, meteorological measurements that had been collected continuously at a measuring station 350 m from the centroid of catchment W_1 were used as climatic data. A total rainfall of 4.4 mm was recorded on August 26, 2023, which followed a 7-day dry period. Precipitation occurred in two stages – the first lasted 10 minutes (from 4:48 to 4:58 a.m.) with 0.2 mm of rain, and the second lasted 90 minutes (from 2:21 to 3:51 p.m.) with 4.2 mm of rain (Figure 3). The instantaneous flow during the entire 4.2 mm precipitation event was measured at outfall W_1 with an accuracy of 1 minute.

2.2.1. Model construction

The detailed subdivision of the area enabled precise delineation of the surface runoff paths, allowing the subcatchments to be properly connected along these paths and according to the slope of the land, as long as there were no drainage inlets on the surface (such as roads or parking places). The polygons generated through geoprocessing allowed for a high level of mapping accuracy in the surface description of the study area.

The empirical modified Horton model was used to calculate the infiltration process. According to Rossman and Huber [2016], this is one of the best-known computational methods for the infiltration process, and it is widely used in rainfall-runoff process modelling [Sofijanic et al. 2022; Li et al. 2015]. Horton's method is considered better suited for single-event simulations compared to the Green-Ampt method [Parnas et al. 2021], while its modified formula provides a more accurate estimation of the infiltration process under low rainfall intensities [Rossman, Simon 2022]. The model is based on calculations consistent with the dynamic wave equations for a 0.5-second routing step for both rainy and dry weather. Time-step restriction was calculated using the formula (1) from the dynamic flow routing model EXTRAN [Roesner et al. 1992]. The shortest sections of gutter pipes determined the routing step value (Δt) to be below 0.8 seconds.

$$\Delta t \leq \frac{L}{(g \cdot D)^{0.5}} \tag{1}$$

where: Δt – time step (sec); L – the pipe length (m); g – gravitational acceleration (9.8 m/sec^2); D – pipe depth (m). The dynamic wave method solves the complete one-dimensional Saint-Venante flow equation, which produces accurate results for phenomena such as backwater, flow reversal, and operation of collectors under pressure [Rossman et al. 2022].

2.2.2. Model calibration

The parameters describing the subcatchments were subjected to the calibration process. For each separated

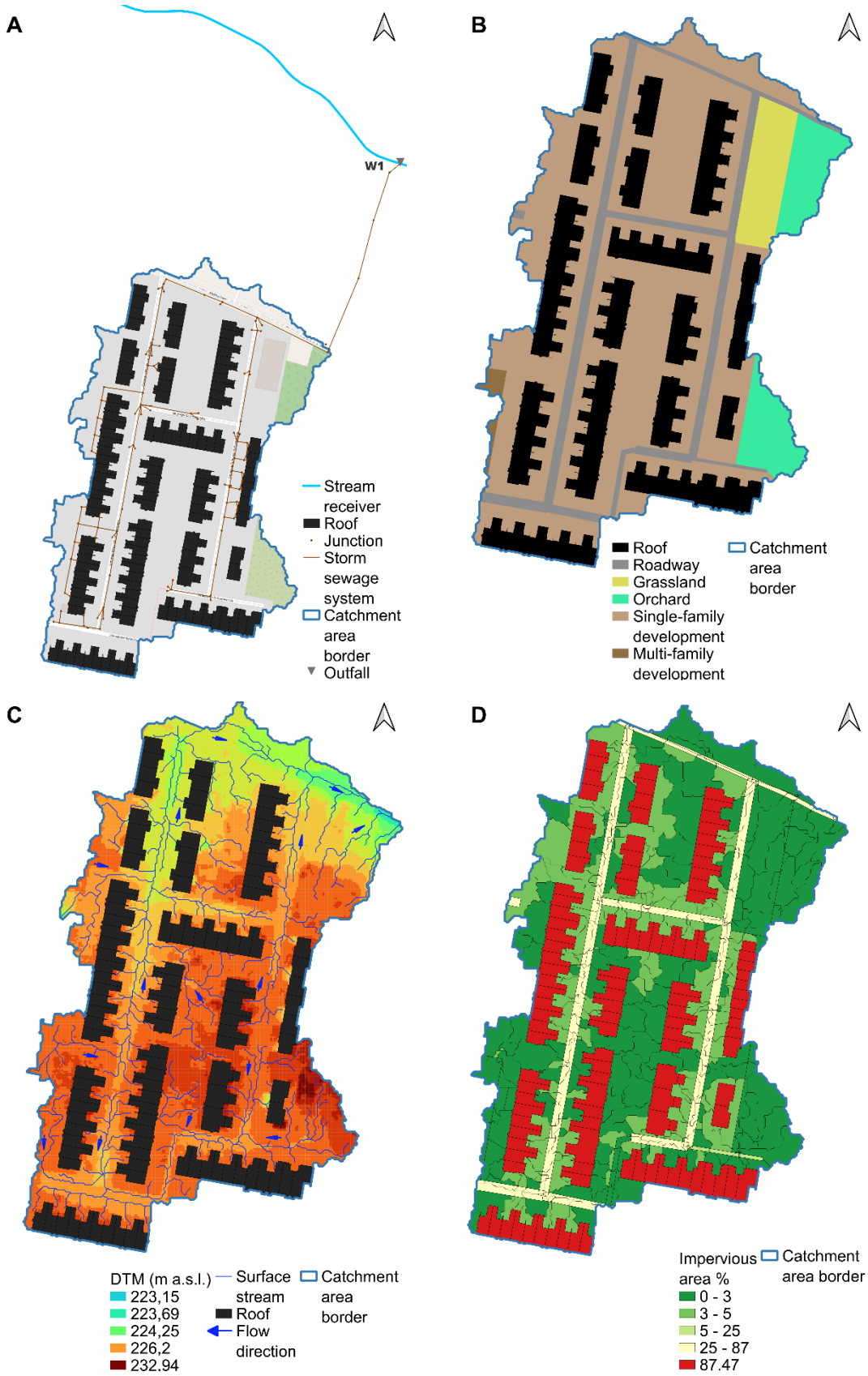

Figure 2. Results of detailed analyses of the study area using available databases: A — route of the drainage system; B — land use; C — elevation and directions of surface water runoff; D — subcatchment imperviousness

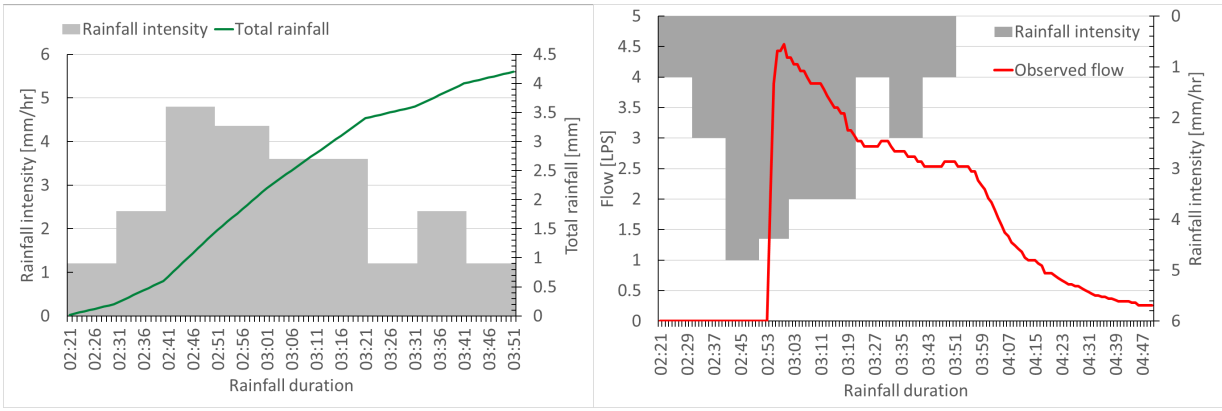

(a) (b)

Figure 3. Rainfall mass curve and hyetograph of 4.2 mm precipitation (a) and flow observed at outfall W_1 (b) used for the calibration process

Table 3. Values of the basic parameters for the land use groups in the study area obtained during the SWMM calibration process

Description	Imperv [%]		N Imperv	N Perv	Dstore Imperv [mm]	Dstore Perv [mm]	Zero Imperv [%]	Width A [m]
	min	max						
Building roofs-BUBD	87.47		0.010	0.045	3.69	3.69	36.00	0.7
Other roadway-SKJZ08	13.1	36.0	0.015	0.300	1.20	5.08	40.00	0.3
Local roadway-SKJZ06	34.6	49.5	0.010	0.300	1.20	5.08	40.00	
Alley-SKRP01	2.0	3.2	0.011	0.280	1.20	5.08	40.00	
Grass vegetation-PTTR01	1.0	2.5	0.140	0.280	5.08	7.62	20.00	0.3
Orchard-PTUT03	1.1	2.88	0.210	0.280	5.08	7.62	20.00	
Single-family dwelling-PTZB02	2.0	4.02	0.105	0.280	5.08	7.62	20.00	

subcatchment, the currently-existing development (according to the Database of Topographical Objects) was extracted using GIS geospatial analysis tools. Separate parameters characterizing the existing surface, such as slope, the proportion of permeable and impermeable surfaces, Manning's roughness coefficients, and retention capacity, were assigned to the prepared polygons. Table 2 lists the values of the basic parameters obtained in the calibration process of the single precipitation phenomena under study. The hydraulic width of the outflow stream [m], which is not a physical parameter, was estimated using formula (2) [Nowogoński et al. 2019].

$$W = A \cdot 1.5 \cdot F^{0.5} \tag{2}$$

where: F is the area [m^2] of a single subcatchment; and A has been calibrated, and its value is given in Table 3, which also includes other values determined during the calibration process:

- Imperv: the percentage of impervious surface within the catchment area;
- N Imperv: factor n for the Manning formula for the impervious part of the catchment;
- N Perv: factor n for the Manning formula for the pervious part of the catchment;
- Dstore Imperv: retention capacity of the impervious surface;
- Dstore Perv: retention capacity of the pervious surface;
- Zero Imperv: percentage of the impervious surface with no retention capacity.

The impervious fractions of the subcatchments were not subjected to the calibration process. The values were determined using a detailed analysis of land cover according to Database of Topographical Objects, along with high-resolution orthophotos and field inspections.
The parameter values were used to determine the correct model response for single precipitation events under the existing conditions. The aim of the calibration was to align the simulated hydrograph with the measured hydrograph. It was important that the total outflow volume, peak discharge, peak time, and rising/falling line matched the

Table 4. The basic measures of fitness coefficients for built SWMM model

Indicator		Description	Formula	Obtained value	Assessment	Literature
NSEC	Nash-Sutcliffe Efficiency Coefficient	Compare the results of model's response and measurement data	$1-\frac{\sum_{t=1}^{T}(Q_o^t-Q_s^t)^2}{\sum_{t=1}^{T}(Q_o^t-\overline{Q_o})^2}$	0.885	-∞ - 1; very good	[Titterington et al. 2017], [Moriasi et al. 2007], [Lin et al. 2017]
ISE	Integral Square Error	The accuracy of the matching between simulated and observed data	$\frac{\sqrt{\sum_{t=1}^{T}(Q_o^t-Q_s^t)^2}}{\sum_{t=1}^{T}Q_o^t}$	0.02	0 – 3; excellent	[Shamsi et al. 2017]
RMSE	Root Mean Square Error	Differences between observed and simulated values	$\sqrt{\sum_{t=1}^{T}(\frac{(Q_o^t-Q_s^t)^2}{T})}$	0.442; < 0.5*1.307	less than half of the standard deviation; good	[Singh et al. 2004], [Moriasi et al. 2007]

measured values as closely as possible. For this purpose, the values of N Imperv, N Perv, Dstore Imperv, Dstore Perv, Zero Imperv, and Parameter A from formula (2) were updated for the subcatchments representing each type of land use. These values for each type of development were selected by gradually adjusting them up or down. The entire process was carried out using a trial-and-error method, with a simulation performed after each parameter change. Based on the results, parameters were calculated for the qualitative assessment of the model, along with a hydrograph plot (Figure 6 for the parameters based on Table 3). Of particular importance in the calibration process were the parameters describing depression Zero Imperv and Dstore Imperv for the impervious parts. The Dstore Imperv and Perv values obtained were close to the range suggested by Endreny [2006].

2.2.3. Model validation

The hydrodynamic model generated continuity errors of 0.0% for surface runoff and 0.0% for flow routing. These values clearly indicated that the model quality was excellent [Rossman et al. 2022]. In the next step, the basic measures of fitness coefficients were calculated to assess the quality of the constructed model. These were used to compare the model's response with the measured data. Table 4 summarises the calculated indicators, along with short comments for each. The symbols used in the formulas are as follows:

Q_o represents the values of the observed outflow (LPS) *(litres per second)*;

Q_s represents the values of simulated runoff (model response) (LPS);

$\overline{Q}_o$ represents the average of the observed runoff (LPS).

When above basic indicators of the model's effectiveness were found to be completely satisfactory, the constructed model for a single precipitation event was considered correctly calibrated.

2.3. GI modelling

The hydrodynamic model allowed for the evaluation of the rainwater drainage system's performance in terms of the amount of rainwater runoff from the studied area in the current conditions (accurate mapping). The model was then modified to simulate the operation of the rainwater drainage network under hypothetical conditions in which the study area incorporates GI facilities, represented in the SWMM as LID. LID objects are typically represented by a combination of correctly defined and characterized layers filled with an assumed type of material.

Following Bond et al. [2021], identical parameters were assumed for the BC facilities embedded in the study area, as shown in Table 5, which remain within the ranges of the parameters presented in Hörnschemeyer et al. [2023], with the exception of the drainage coefficient parameter. The LID facilities were differentiated only by the location of the installation and the individual area. In addition, it was assumed that the entire newly inserted subcatchment was occupied by the indicated LID object (the SWMM allows the separation of the LID surface within the selected subcatchment).

The drainage coefficient parameter is defined as the rate of water outflow through the drainage system and described as a function of the water height in the retention layer above the drainage outlet [USEPA 2022]. Therefore, formula (3), used in Lee et al. [2018] and described in the Drain Advisor, was applied. For a time of $T = 12$ hours and

Table 5. Summary of the LID parameters used in the calibrated SWMM model according to [Bond et al. 2021]

Layer	Parameter	Unit	Bio-retention cells (BC)
Surface layer	Berm height	mm	250
	Vegetation volume	share	0.1
	Surface roughness	–	0.3
	Surface slope	%	1
	Swale Side Slope	run/rise	–
Soil layer	Thickness	mm	600
	Porosity	share vol.	0.45
	Field capacity	share vol.	0.121
	Wilting point	share vol.	0.057
	Conductivity	mm/hr	91
	Conductivity slope	–	44
	Suction head	mm	50
Storage layer	Thickness	mm	400
	Void ratio	voids/solids	0.54
	Seepage rate	mm/hr	2.6
	Clogging factor	–	0
Drain	Flow coefficient	mm/hr	5.4*
	Drain exponent	–	0.5
	Offset height	mm	200

* The parameter was calculated using formula (3)

a height of D = 1250 mm minus an offset of 200 mm, the flow coefficient was estimated to be 5.4 mm/hr.

$$q_{coeff} = \frac{2 \cdot D^{0.5}}{T} \tag{3}$$

where: D – the height of the layers above the drain outlet minus the offset (mm); and T – drainage time (h).

Figure 4 presents a proposal for the implementation of selected LID devices for the existing housing estate under consideration. The cadastral division of land (boundaries of cadastral plots) and the layout of the existing underground infrastructure, excluding rainwater drainage, were omitted, as was any street furniture. When conceptualizing the layout of the LID infrastructure, the provisions of a technical catalogue [Iwaszuk et al. 2019] regarding the area requirements of selected LID structures were taken into account. For BC, the minimum required area was 1% of the drained catchment area. The selected grassy green areas offer opportunities for practical LID implementation, which, combined with underground and above-ground drainage systems, can increase the residents' living comfort [Liu et al. 2022] and improve rainwater management.

Rain gardens equipped with a drainage system (represented in SWMM as "bio-retention cells BC") connected to the existing rainwater drainage network were selected. A total of 32 LID facilities covering 0.474 ha were applied. Line BC systems (16 pcs, with a total area of 0.459 ha) formed the main surface runoff routes approximately 3.8 m wide, and were located in existing biologically active areas. The largest was 836 m^2, while the smallest was 70 m^2. Street BC (16 pcs, with a total area of 0.015 ha) were built along roads with a total area of 9.2 m^2. Where conditions allowed, excess overflows from the LID systems were connected to the downstream and adjacent LID systems, or alternatively, to the existing rainwater drainage network.

3. RESULTS

The total rainwater runoff at outfall W_1 was 14.4 m^3 (measured) and 15.2 m^3 (simulated). Pearson's correlation coefficient (r) was 0.965, while the coefficient of determination (R^2), which indicates the collinearity between the time series of measured and simulated flows, was calculated to be 0.9319. Since this value was close to unity, it demonstrates a high level of convergence between the simulated and measured flow results (Figure 5).

Figure 4. Illustration of the implementation of green infrastructure (BC) in the study area of an existing housing estate.

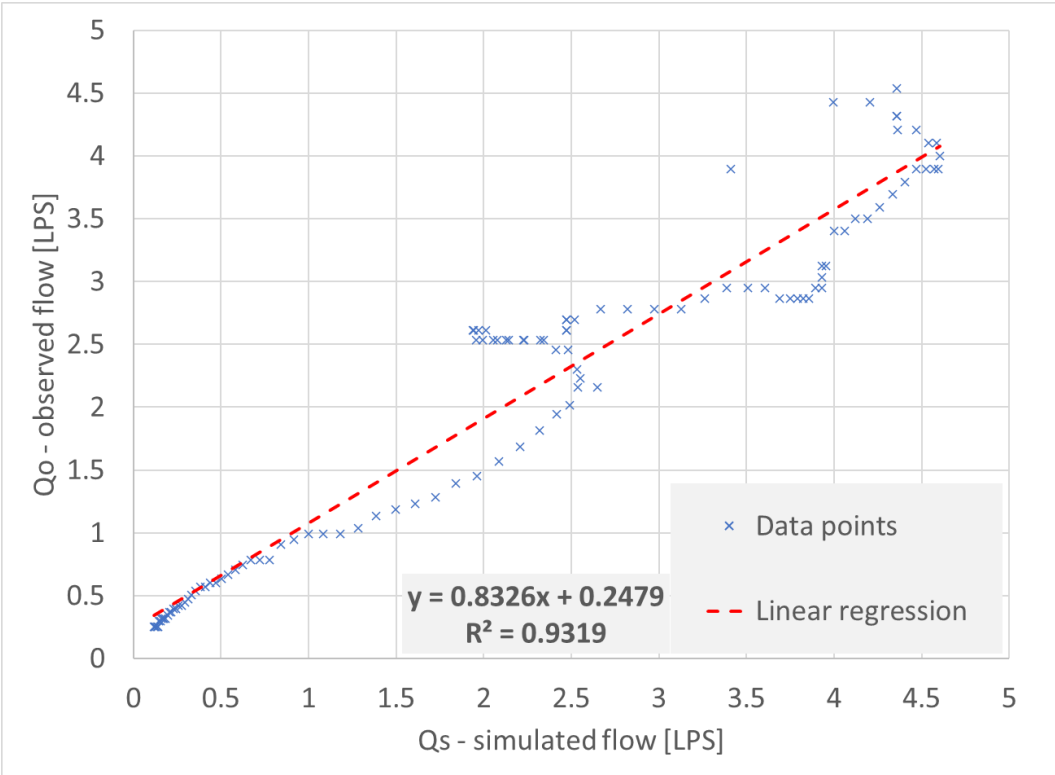

Figure 5. Linear regression plot of R2 for a dataset of the measured rainwater flow (Q_o) at outfall W_1 and the simulated value (Q_s) based on the SWMM

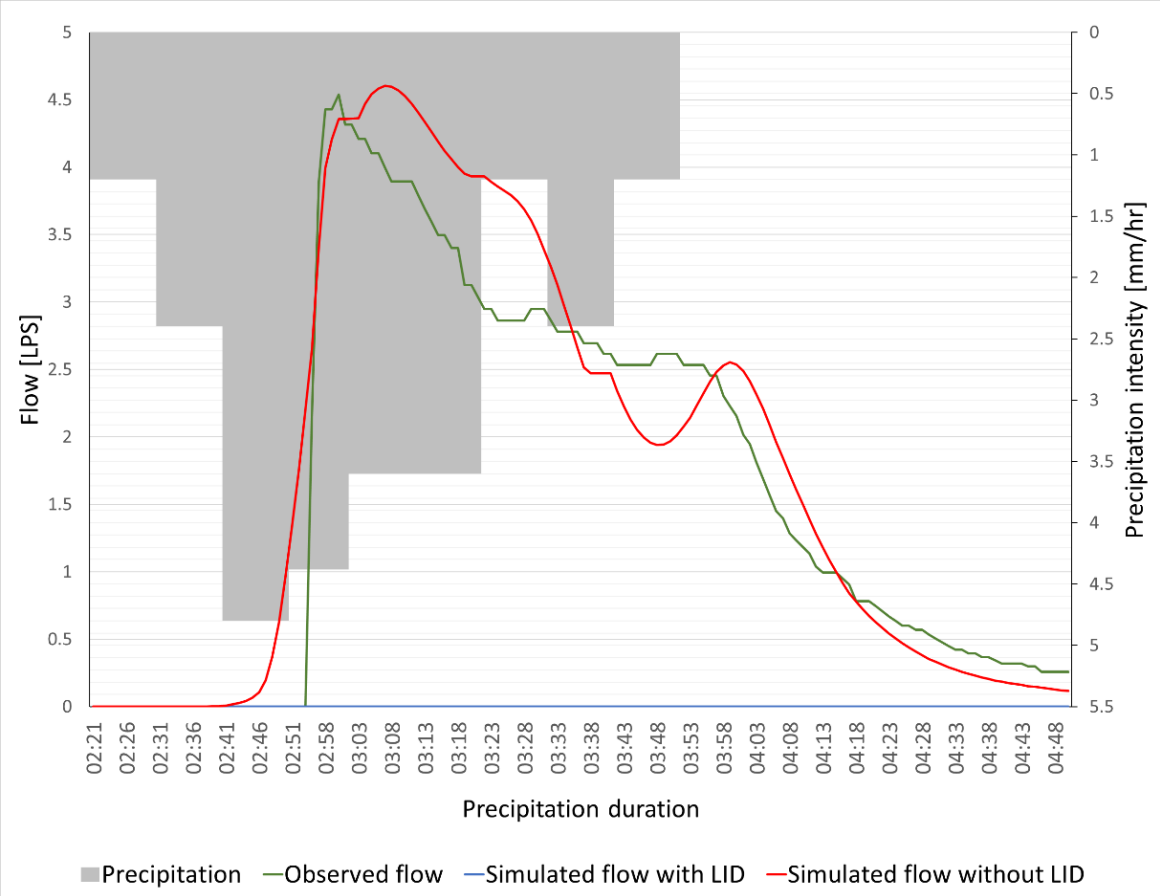

Figure 6. Flow observed at outfall W_1 on August 26, 2023, along with the modelling results for the existing conditions, and for the scenario with the selected LID equipment implemented

The results of the single-event modelling of the observed real precipitation showed a significant reduction in runoff at the tested outfall W_1 with the implementation of LID. The average value of simulated instantaneous flows was 2.21 LPS (litres per second), compared to the measured flows of 2.09 LPS, with standard deviations of 1.516 and 1.307 LPS, respectively. The measured peak flow was 4.54 LPS, recorded at 3:00 p.m., while, according to the SWMM, the maximum flow occurred at 3:07 p.m. and amounted to 4.35 LPS. The flow rate simulated for the existing conditions, measured on August 26, 2023, is illustrated in Figure 6, which also shows the model's response in the case of LID implementation in the housing estate under study, assuming no outflow.

3.1. Total volume and peak flow reduction

The simulation results for scenarios S_0 – S_7 are summarized in Table 6. The findings demonstrated a significantly positive impact of LID infrastructure on the total volume of rainwater in the drainage system in the studied area, achieving an average reduction of 86% across scenarios S_1 – S_7. The rate of total runoff reduction (LID vs. non-LID) decreased as the duration and total rainfall increased, with a minimum reduction value of 78% in scenario S_7 and a maximum of 95% in scenario S_1.

Meanwhile, the implemented LID facilities reduced peak flows by an average of 94%, with a maximum of 96% in scenario S_1 and a minimum of 93-94% for scenarios S_2–S_7. In this case, there was no significant increase in reduction relative to the duration of the rainfall. The above results exclude the real precipitation in scenario S_0, where the reduction in both total runoff and peak flow was 100%.

The graph in Figure 7 presents the average total volume and peak flow reduction as a function of precipitation duration. Here, the effectiveness of LID facilities in reducing rainwater runoff at the proposed locations in the area under study decreased relative to the entire existing drainage system and depended on the average intensity and duration of precipitation. As indicated by high R^2 values, the reduction followed the polynomial trend lines that had been determined.

Table 6. The simulation results of the calibrated model for the entire study area at the sewer outfall for scenarios S_0–S_7

	Scenario S_0	Scenario S_1	Scenario S_2	Scenario S_3	Scenario S_4	Scenario S_5	Scenario S_6	Scenario S_7
no LID								
Max flow [LPS]	4.6	449.2	464.0	454.8	393.1	359.3	349.9	266.2
Total volume [m³]	17	539	752	916	953	1008	1072	1139
with LID								
Max flow [LPS]	0.0	17.5	31.6	31.7	25.2	22.6	22.1	17.6
Total volume [m³]	0	29	56	111	134	167	204	246
reduction								
Max flow [LPS]	100%	96%	93%	93%	94%	94%	94%	93%
Total volume [m³]	100%	95%	93%	88%	86%	83%	81%	78%

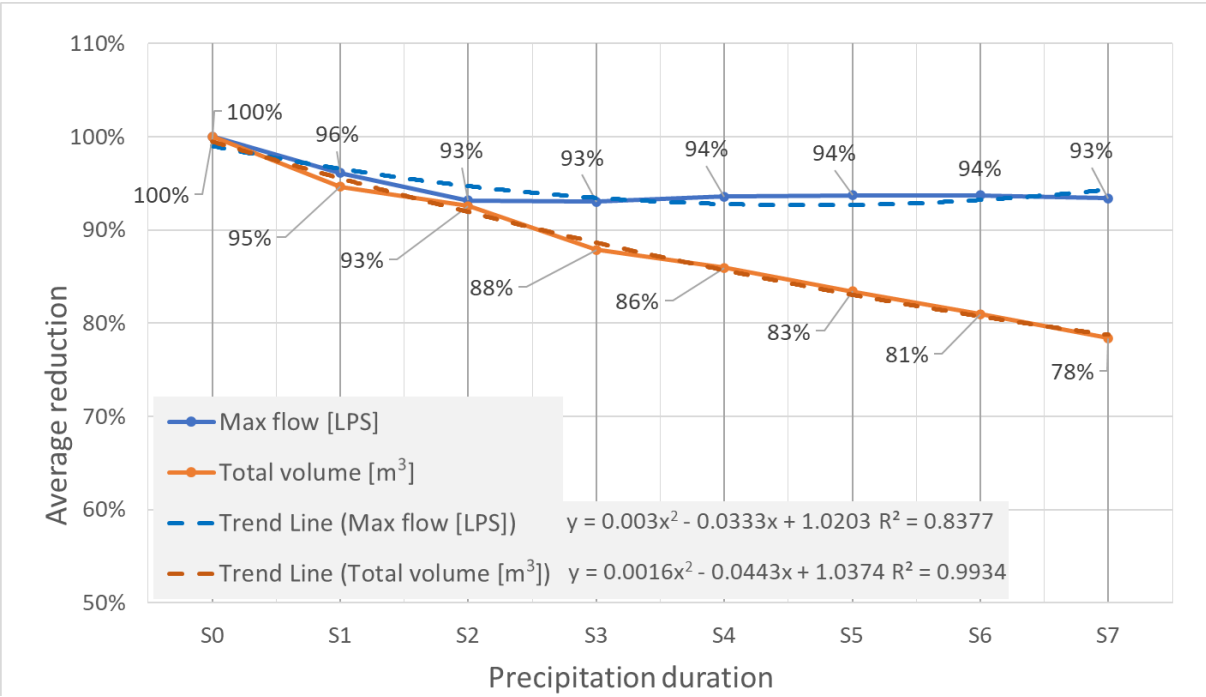

Figure 7. *Average reductions in the total volume and peak flow for scenarios* S_0–S_7

3.2. Storage volume of LID facility

Considering the volume of rainfall in the studied catchment in relation to the calculated retention volume at all LID facilities, the percentage of LID storage was in the range of 28–37% (32% on average) of the total synthetic rainfall volume, as shown in Figure 8.

Considering the rainfall volume of 365 m³ that fell on the surface of the study catchment on the day of the measurement, and the estimated LID retention volume of 41 m³, the percentage of rainfall volume retained by LID was 11%. It should be noted that SWMM separates initial and final storage in its summary report, with the difference between these volumes representing the potential rainwater retention volume. In this study, LID storage was absolutely dependent on the adopted LID parameters (Table 5), and the initial layer was approximately 187 m³.

The inflow values shown in Table 4 must be reduced by the amount of infiltration (average 0.033 m³/m²) and evaporation (average 0.0036 m³/m²), which depend on the local soil and atmospheric conditions, as well as the precipitation duration. The difference between rainfall depth and LID storage reflected the total volume of rainwater that either flowed through the LID (surface and drain outflow) or bypassed it. This figure was influenced by many factors, including as depression storage, LID

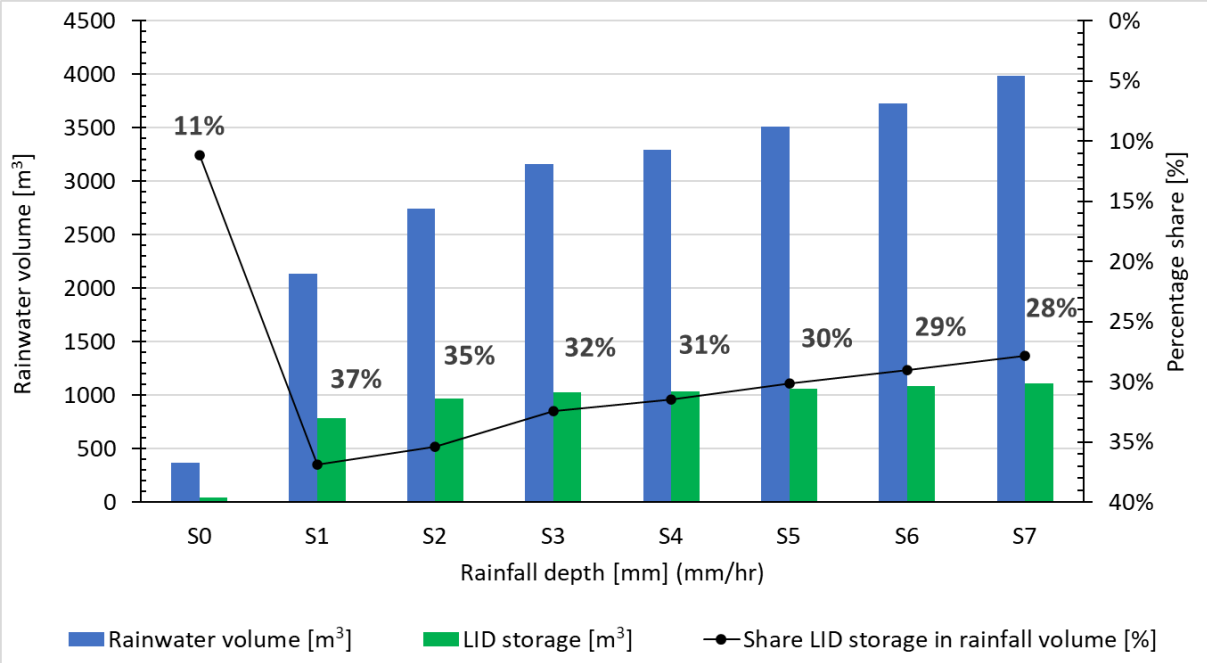

Figure 8. Percentage distribution of the rainwater volume and storage volume of LID facility as a function of rainfall depth

Table 7. Summary of the simulation results of the calibrated SWMM for individual LID facilities implemented in the study area for scenarios S_0–S_7

Scenario	S_0	S_1	S_2	S_3	S_4	S_5	S_6	S_7
Total Inflow (m³)	37.9	658.2	987.1	1234.8	1304.7	1404.0	1512.8	1629.2
Surface and Drain Outflow (m³)	0.0	32.7	133.6	273.6	318.7	385.4	458.9	538.8
Average inflow (L/m²)	0.008	0.139	0.208	0.260	0.275	0.296	0.319	0.344
Average outflow (L/m²)	0.000	0.007	0.028	0.058	0.067	0.081	0.097	0.114
Average reduction (%)	**100**	**95**	**86**	**78**	**76**	**73**	**70**	**67**

structure, evaporation and infiltration. The maximum calculated LID retention volume was approximately 1100 m³ (for scenario S_7).

3.3. Hydrological performance of LID facilities

Table 7 presents the results of quantitative calculations illustrating the performance of individual LID facilities. Key values, such as total inflow, surface outflow and drain outflow, are given in m³. These represent the total rainwater flowing into the LID, and the total rainwater flowing out through the drainage system or overflowing to the drainage system, respectively. The indicated LID areas represent the minimum and maximum facility sizes, while the sum indicates the overall area of installed LID.

The average inflow and average outflow were calculated based on individual inflows and outflows per unit area (L/m²). The calculated average reductions in surface runoff indicated the high efficiency of the applied LID solutions. The efficiency of rainwater surface runoff reduction ranged from 67% to 95% for scenarios S_1–S_7, with an average of 78% with a standard deviation of 9%.

The total inflow in in Table 7 represents the volume of water flowing into the LID. The difference between the rainwater volume and the total inflow into the LID accounts for all types of losses, and takes into account the surface characteristics; pervious and impervious depression storage; the impervious fraction of subcatchments; and infiltration and evaporation along the surface runoff path.

The graphs presented below show the effectiveness of reducing the total inflow (L/m²) of rainwater using LID in the studied housing estate for all scenarios, considering all 32 LID units (Figure 9). These values were calculated by assuming the total inflow of rainwater from all surface types into a single LID, as well as the *drain outflow* – the total outflow always directed to the rainwater drainage system

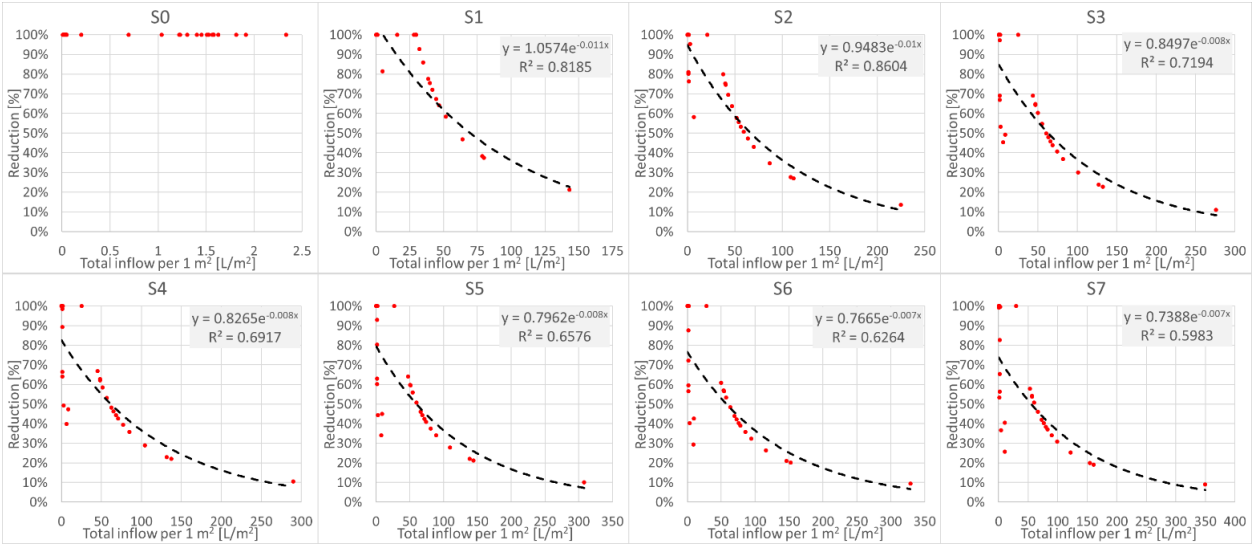

Figure 9. Dependence of the total inflow per 1 m2 and reduction in rainwater for BC cells in the residential area under study for scenarios S_0–S_7

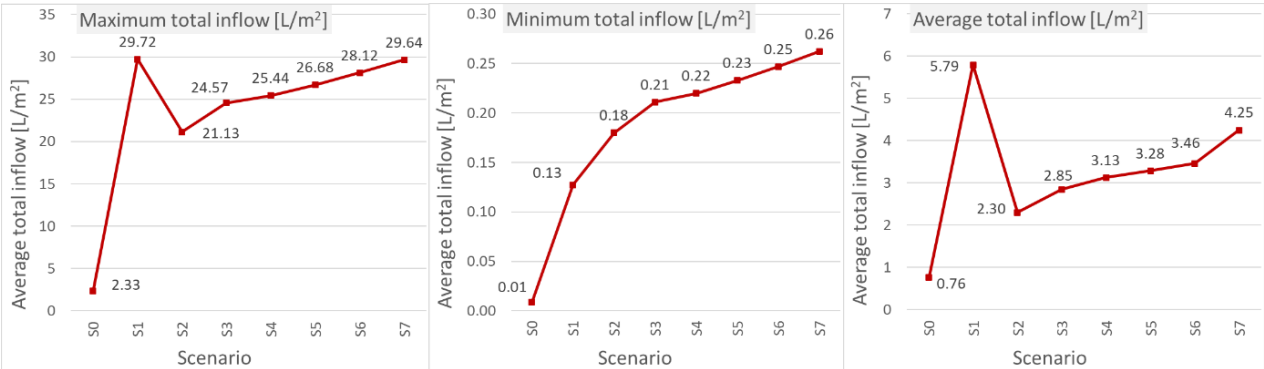

Figure 10. Maximum, minimum and average values of the rainwater inflow limit [L/m2] per 1 m2 of surface area of LID facilities for scenarios S_0–S_7 for which there was a 100% quantitative reduction of inflow

– and the *surface outflow* – the outflow of excess water directed to an LID located downstream or, alternatively, into the rainwater drainage system.

Figure 9 illustrates the unit inflow reductions for BC (red points) for which there were exponential trend lines with a statistically significant coefficient of determination (R^2) for $\alpha \leq 0.05$, demonstrating the relationship between reduction and total inflow. The flattening of this line was clearly noticeable for shorter precipitation periods (S_1, S_2). For longer precipitation events, characterized by lower intensities, there was a systematic decrease in rainfall-runoff reduction.

These analyses also revealed the limit values at which BC reduced the entire inflow, clearly determined by the duration and intensity of precipitation. Figure 10 details these limit values, including the minimum, maximum and average fully reduced rainwater inflows per 1 m² of the LID facility area. For precipitation in scenario S_2, with an average intensity of 175.33 LPS/ha, the values of average fully reduced inflows at LID were revealed to be the lowest at 2.30 L/m² (excluding real rainfall). In contrast, in scenario S_1, BC were loaded with the largest tributary inflows, which were fully reduced.

The highest and most fully-reduced values of inflow per unit area of LID occurred for heavy rainfall in scenario S_1, amounting to 29.72 L/m² (with an average of 5.79 L/m²). During the first phase of long-term precipitation, the LID layers saturated slowly, thus increasing the volume of retained rainwater with slight simultaneous infiltration into the native soil. Over time, the water storage capacity decreased, but infiltration into the ground increased. When the retention volume of the LID was exceeded, excess water was diverted to the rainwater drainage system, which also reached its maximum hydraulic capacity, followed by surface outflow of rainwater.

Table 8. Summary of the results obtained for the considered precipitation scenarios S_0–S_7

No.	Scenario	S_0	S_1	S_2	S_3	S_4	S_5	S_6	S_7
	share LID storage in rainfall volume								
1A	Rainwater volume [m³]	365	2137	2742	3156	3296	3510	3725	3984
1B	Final LID storage [m³]	41	788	970	1024	1036	1057	1081	1108
1	**Average share [%]**	**11%**	**37%**	**35%**	**32%**	**31%**	**30%**	**29%**	**28%**
	LID hydrological performance								
2A	Average inflow [L/m²]	0.008	0.139	0.208	0.260	0.275	0.296	0.319	0.344
2B	Average outflow [L/m²]	0.000	0.007	0.028	0.058	0.067	0.081	0.097	0.114
2	**Average reduction [%]**	**100%**	**95%**	**86%**	**78%**	**76%**	**73%**	**70%**	**67%**
	average total inflow to LID with full reduction								
3	**Fully reduced inflow [L/m²]**	**0.76**	**5.79**	**2.30**	**2.85**	**3.13**	**3.28**	**3.46**	**4.25**
	total outfall volume reduction								
4A	Total volume [m³]	17	539	752	916	953	1,008	1,072	1139
4B	Reduced volume [m³]	0	29	56	111	134	167	204	246
4	**Average reduction [%]**	**100%**	**95%**	**93%**	**88%**	**86%**	**83%**	**81%**	**78%**
	outfall peak flow reduction								
5A	Peak flow [LPS]	4.60	449.16	464.03	454.78	393.10	359.34	349.85	266.20
5B	Reduced peak flow [LPS]	0.00	17.51	31.63	31.66	25.19	22.57	22.05	17.58
5	**Average reduction [%]**	**100%**	**96%**	**93%**	**93%**	**94%**	**94%**	**94%**	**93%**

This shows that LID were more effective in reducing the total inflow during short and heavy precipitation events. However, for scenario S_7, a slow and systematic increase in the maximum and average total inflow was observed, reaching a value similar to scenario S_1 (29.64 L/m²). This ability to accept more inflow water and fully reduce it during long-term rainfall can be explained by the increase in infiltration.

The results of the study are summarised in Table 8 below.

Pearson's linear correlation coefficients were calculated for the results that were statistically significant. The strongest direct proportional correlation (0.98) was found between the results of no. 2 and no. 4, while a weaker relationship (0.80) was observed between no. 2 and no. 5. A significant correlation (0.83) was observed for no. 1 and no. 5B. The weakest relationships were found for no. 3, although there was a significant correlation (0.69) between no. 3 and no. 1. An inversely proportional relationship (-0.76) was found between no. 1 and no. 5.

4. DISCUSSION

Proper model calibration, based on the measured data from a single real precipitation event, allowed for the accurate reproduction of the conditions prevailing in the study area. The runoff-run-on process was modelled for a single actual precipitation event (S_0), as well as for conditions prevailing in hypothetical scenarios (S_1–S_7) and for alternative rainwater management using GI. Due to the lack of sufficient verification data, single-event calibration and basic measures of model response fitness coefficients were used. This approach ensured an accurate reproduction of the peak value and shape of the hydrograph, while continuous calibration provided a more accurate estimate of runoff volume over time [Rezaei et al. 2019].

The simulations carried out as part of this study proved that the implementation of GI results in a significant reduction in both peak flow and runoff volume of rainwater. According to [Golden et al. 2018], LID can help achieve many hydrological objectives, such as reducing peak flow and restoring natural surface flow and infiltration to the original conditions (i.e., those existing before an area underwent human development).

In this paper, it has been demonstrated that for the outfall, W_1, of the entire drainage system, an average total volume reduction of 86% and a peak flow reduction of 94% can be achieved with GI covering approximately 10% of the catchment drainage area. The inclusion of this 10% GI area in the structure of the housing estate did not change its functionality or spatial arrangement. The analyses showed that the efficiency of reducing rainwater surface runoff in BC ranged between 67% and 95%. Most importantly, the efficiency of BC is highest for intense and short (15 min) rainfall events, reaching a 95% reduction in runoff volume. Similarly high reductions, exceeding 97%, were reported in a seven-year study of a rain garden in Xi'an, China [Guo et al. 2019], and in a one-year observation of a rain garden in North Carolina, USA, where 78% of the water either exfiltrated the cell or left via evapotranspiration

[Hunt et al. 2006]. Other studies have also reported high volume reductions, ranging from 43 to 94% [Mai et al. 2019], from 37 to 61% [Jiang et al. 2015], and reaching 50% [Christensen et al. 2012]. However, these studies mainly involved field sampling and laboratory analysis.

The saturation of rainwater storage layers leads to a decreasing reduction in total volume as rainfall duration increases, reaching a minimum value of 67% for a three-hour rainfall. Taking into account rainfall intensity, the runoff reduction efficiency from the simulations decreases as total rainfall increases. The study also indicated that GI is more effective in reducing total inflow and peak flow for high-intensity heavy rainfall events that are shorter than 30 minutes.

It should be noted that the layered structure of the applied LID, which determined the course of the infiltration, retention, and evaporation processes, was assumed and constant in the simulations. The materials and plants used in the LID can also influence the rate and effectiveness of rainwater inflow reduction. The results obtained were a consequence of the adopted structural parameters of individual LID layers. These parameters determined the LID final storage capacity, which was approximately 1100 m^3 and accounted for an average of 28% of the total rainfall volume. For such values, a 67% reduction in total inflows to the BC was achieved. The value of the reduction increases with the increasing LID storage in the rainfall volume, reaching a 95% reduction for 37%.

As a result of the analyses, the relationship curves of the total inflow per 1 m^2 and the outflow reduction were developed, which could help in the selection of BC facilities and in the estimative calculation of the amount of rainwater that does not enter the drainage system. Detailed analyses of individual LID facilities revealed a strong relationship (R^2 = 0.5983–0.8185) between the total inflow per 1 m^2 and the reduction in rainwater, with the highest value occurring for 15 minutes of rainfall. The relationship weakened as the duration of rainfall increased. The minimal fully quantitative reduction of the average inflow to LID of 2.30 L/m^2 was noted for 30 min of precipitation (S_2), whereas the maximum reduction of 5.79 L/m^2 was observed for 15 min of precipitation (S_1).

This could be explained by the analysis of the percentage distribution between rainfall volume and retention volume. Under the assumed parameters, individual LID sites reached the maximum storage layer charge after approximately 30 min of rainfall. Therefore, once this time threshold was exceeded, rapid surface and drain runoff occurred, resulting in a more than a two-fold decrease in inflow reduction.

Detailed databases, high-precision and accurate subcatchment delineation, and calibration using a single flow measurement at outflow W_1 allowed for the matching of the hydrographs of measured and simulated flows. Obviously, the inclusion of more measurement data from additional control sites would reduce this model's uncertainty. The construction of LID in an existing development is a complex task due to numerous constraints. This type of solution should be developed at the concept, design and construction stages. These efforts will contribute to more effective protection of rainwater recipients on both qualitative [Smith et al. 2023] and quantitative [Guo et al. 2013] scales. It has been pointed out that methods for measuring and optimising the performance of integrated multifunctional green infrastructure have not been fully developed [Wang et al. 2020]. This study has attempted to estimate the hydrological performance of the LID at one selected site.

The complex interdependency of the individual LID performance parameters in the system under study highlights opportunities for future studies that could introduce additional factors, such as an altered LID structure. The hydrological performance of the LID discussed here, and rainwater reduction values of the entire system, should also be verified using other precipitation phenomena occurring in the study area and the introduction of new calibration points. In addition, future modifications could include scenarios involving varying LID locations. Further research is necessary due to the lack of detailed technical loading parameters for the relationship between LID and precipitation.

5. SUMMARY

The parameters and indicators discussed above highlight the dependencies that are crucial for the effective operation of the BC equipment. Their interpretation enables a comprehensive assessment of the functionality of the GI solutions implemented in the area under study. It is evident that both the average inflow to the LID, and the total volume discharged at the outfall, significantly depend on rainwater volume. The outfall of total volume reduction at the discharge point of the sewer system is most significantly determined by the efficiency of the LID operation, specifically the average outflow from the LID. However, reduction in peak flow at the outfall is also most closely linked to the percentage of LID storage in rainfall volume. Thus, the structure of individual BC unit layers determines the reduction of peak flow, while the amount of inflow, and its reduction in individual LID units, define the rainwater volume reduction at the outfall. There is also a relationship between the reduction in total inflows in BC devices and the LID volume, but it is not sufficiently strong. The aforementioned interdependencies determine the effectiveness of total volume and peak flow reduction at the drainage outlet. At the outset of the study, it was believed that the ultimate efficiency of using distributed GI facilities, including the rain gardens under analysis that were equipped with drainage systems, should be the overriding criterion for their selection, considering the structure of individual layers and their location in the area to be drained. Obviously, while the location (which was not analysed in this study) in areas of existing development is very limited, the structure and interconnection of these facilities perform a very important function in the overall system. The analyses indicated that the reductions in

both total volume (78–95%) and peak flow (93–96%) at the system outlet were greater than the inflow-outflow reductions for the individual LID devices (67–95%). This can be explained by the fact that the devices are connected within a cohesive system, where the outflow from an overflowing LID is often intercepted by the next device downstream. This relationship is particularly evident for long-duration rainfall events.

Correct conclusions based on simple relationships between individual phenomena can have a significant impact on the correct management of rainwater in urbanised areas. Such summaries and databases could support the development of guidelines for engineers and urban planners, while also contributing to environmental benefits both locally and on a broader scale.

Verified hydrological performance parameters need to be incorporated into planning, design and strategy documents [Muszyński et al. 2022]. In the context of a changing climate, these documents must strive to achieve the targets set out in the provisions of the European Green Deal [Tache et al. 2023] and the Sustainable Development Goals (SDGs). Therefore, it is considered that a portion of the currently required minimum of 40–60% of biologically active area should be allocated to the development of GI [Resolution… 2018]. In addition, it is proposed that GI should be designed with the goal of minimizing both the total volume and peak flow of rainwater.

REFERENCES AND LEGAL ACTS

AGARWAL S., KUMAR S. 2019. Applicability of SWMM for semi Urban Catchment Flood modeling using extreme Rainfall Events. International Journal of Recent Technology and Engineering (IJRTE) 8, 2: 245–251. DOI: 10.35940/ijrte.A3169.078219.

ARJENAKI M., SANAYEI H., HEIDARZADEH H., MAHABADI N. 2020. Modeling and investigating the effect of the LID methods on collection network of urban runoff using the SWMM model (case study: Shahrekord City). Modeling Earth Systems and Environment 7:1–16. DOI:10.1007/s40808-020-00870-2.

BAI Y., ZHAO N., RUOYU Z., ZENG X. 2019. Storm Water Management of Low Impact Development in Urban Areas Based on SWMM. Water 11, 1: 33. DOI:10.3390/w11010033.

BARSZCZ M. 2017. Zastosowanie modelu SWMM do obliczenia przepływów i ich redukcji przez zbiorniki na obszarze lotniska Chopina [Application of the SWMM model to calculate flows and their reduction through reservoirs in the area of Chopin Airport]. Acta Sci. Pol. Architectura 16, 1: 79–91. ISSN 1644-0633, DOI:10.22630/ASPA.2017.16.1.08.

BATALINI DE MACEDO M., FERREIRA DO LAGO C. A., MENDIONDO E. M., BORGES DE SOUZA V. C. 2018. Performance of bioretention experimental devices: contrasting laboratory and field scales through controlled experiments. Revista Brasileira de Recursos Hídricos Brazilian Journal of Water Resources Versão (RBRH) Porto Alegre, 23, 3. DOI:10.1590/2318-0331.0318170038.

BOND J. 2021. Modeling a Bioretention Basin and Vegetated Swale with a Trapezoidal Cross Section using SWMM LID Controls. Journal of Water Management Modeling 29: C474, CHI 2021. DOI:10.14796/JWMM.C474.

BURSZTA-ADAMIAK E., BINIAK-PIERÓG M., DĄBEK P. B., STERNIK A. 2023. Rain garden hydrological performance – Responses to real rainfall events. Science of the Total Environment 887: 164153. DOI:10.1016/j.scitotenv.2023.164153.

BURSZTA-ADAMIAK E., MROWIEC M. 2013. Modelling of green roofs' hydrologic performance using EPA's SWMM. IWA Publishing Water Science & Technology 68,1: 36–42. DOI:10.2166/wst.2013.219.

CHOI C., BERRY P., SMITH A. 2021. The climate benefits, co-benefits, and trade-offs of green infrastructure: A systematic literature review. Journal of Environmental Management, 291, 1 August 2021: 112583. DOI:10.1016/j.jenvman.2021.112583.

CHRISTENSEN D., SCHMIDT A. R. 2012. An Approach to Analyze the Hydrologic Effects of Rain Gardens. In Low Impact Development for Urban Ecosystem and Habitat Protection, pp. 1–9, DOI:10.1061/41009(333)1.

CIPOLLA S. S., MAGLIONICO M., STOJKOV I. 2016. A long-term hydrological modelling of an extensive green roof by means of SWMM. Ecological Engineering 95, October 2016: 876–887. DOI:10.1016/j.ecoleng.2016.07.009.

D'AMBROSIO R., BALBO A., LONGOBARDI A., RIZZO A. 2022. Re-think urban drainage following a SuDS retrofitting approach against urban flooding: A modelling investigation for an Italian case study. Urban Forestry & Urban Greening 70: 127518. DOI:10.1016/j.ufug.2022.127518.

DAS P., BEHERA M. D., PATIDAR N., SAHOO B., TRIPATHI P., BEHERA P. R., SRIVASTAVA S. K., ROY P. S., THAKUR P., AGRAWAL S. P., KRISHNAMURTHY Y. V. N. 2018. Impact of LULC Change on the Runoff, Base Flow and Evapotranspiration Dynamics in Eastern Indian River Basins during 1985–2005 Using Variable Infiltration Capacity Approach. Journal of Earth System Science 127, 2: 19. DOI:10.1007/s12040-018-0921-8.

DĄBROWSKI W., NOWAK M. 2022. Potential of storm water storage tank outflow construction in the prevention of sewerage overload. Applied Water Science Volume 12: 205, DOI:10.1007/s13201-022-01729-w.

DEL GIUDICE G., PADULANO R. 2016. Sensitivity Analysis and Calibration of a Rainfall-Runoff Model with the Combined Use of EPA-SWMM and Genetic Algorithm.

Acta Geophysica 64, 5: 1755–1778. DOI:10.1515/acgeo-2016-0062.

ENDRENY T. A. 2006. Land Use and Land Cover Effects on Runoff. Processes: Urban and Suburban Development. Encyclopedia of Hydrological Sciences (M.G. Anderson and J.J. McDonnell, eds). John Wiley & Sons, Ltd. DOI:10.1002/0470848944.hsa122.

EPPS T., HATHAWAY J. 2019. Using spatially-identified effective impervious area to target green infrastructure retrofits: A modeling study in Knoxville, TN. Journal of Hydrology 575: 442–453. DOI:10.1016/j.jhydrol.2019.05.062.

GODYŃ I., BODZIONY M., GRELA A., MUSZYŃSKI K., PAMUŁA J. 2023. Determination of Pollution and Environmental Risk Assessment of Stormwater and the Receiving River, Case Study of the Sudół River Catchment, Poland. International Journal of Environmental Research and Public Health 20, 1: 504. DOI:10.3390/IJERPH20010504.

GODYŃ I., GRELA A., MUSZYŃSKI K., PAMUŁA J. 2024. The Impact of Green Infrastructure on the Quality of Stormwater and Environmental Risk. Sustainability 16: 8530. DOI:10.3390/su16198530.

GOLDEN H. E., HOGHOOGHI N. 2018. Green infrastructure and its catchment-scale effects: an emerging science. WIREs Water 5, 1: 1254. DOI:10.1002/wat2.1254.

GRANADOS-OLIVAS A., ALATORRE-CEJUDO L.C., ADAMS D., SERRA Y.L., ESQUIVEL-CEBALLOS V.H., VÁZQUEZ-GÁLVEZ F.A., GINER M.E., EASTOE C. 2016. Runoff Modeling to Inform Policy Regarding Development of Green Infrastructure for Flood Risk Management and Groundwater Recharge Augmentation along an Urban Subcatchment, Ciudad Juarez, Mexico. Journal of Contemporary Water Research & Education, 159: 50–61, DOI:10.1111/j.1936-704X.2016.03229.x.

GRUMBLES B. 2007. Memorandum: Using Green Infrastructure to Protect Water Quality in Stormwater, CSO, Nonpoint Source and other Water Programs (United States Environmental Protectional Agency Office of Water, 05.03.2007).

GUGiK, Head Office of Geodesy and Cartography. Available online: https://www.gov.pl/web/gugik/dane-pzgik4 (accessed on September 2023).

GUO Q., CORREA C. A. 2013. The Impacts of Green Infrastructure on Flood Level Reduction for the Raritan River: Modeling Assessment. World Environmental and Water Resources Congress 2013: Showcasing the Future - Cincinnati, OH, United States, 19 May 2013. DOI:10.1061/9780784412947.035.

GUO C., LI J., LI H., LI Y. 2019. Influences of stormwater concentration infiltration on soil nitrogen, phosphorus, TOC and their relations with enzyme activity in rain garden. Chemosphere 233: 207–215, DOI:10.1016/j.chemosphere.2019.05.236

HAMOUZ V., MØLLER-PEDERSEN P., MUTHANNA T. M. 2020. Modelling runoff reduction through implementation of green and grey roofs in urban catchments using PCSWMM. Urban Water Journal 17, 9: 813–826. DOI:10.1080/1573062X.2020.1828500.

HÖRNSCHEMEYER B., HENRICHS M., DITTMER U., UHL M. 2023. Parameterization for Modeling Blue–Green Infrastructures in Urban Settings Using SWMM-UrbanEVA. Water, 15, 15: 2840, DOI:10.3390/w15152840.

HUNT W. F., JARRETT A. R., SMITH J. T., SHARKEY L. J. 2006. Evaluating Bioretention Hydrology and Nutrient Removal at Three Field Sites in North Carolina. Journal of Irrigation and Drainage Engineering ASCE 132: 600–608. DOI:10.1061/(ASCE)0733-9437(2006)132:6(600)

HUANG Y., TIAN Z., KE Q., LIU J., IRANNEZHAD M., FAN D., HOU M., SUN L. 2020. Nature-based solutions for urban pluvial flood risk management. WIREs Water 2020, 7; e1421, DOI:10.1002/wat2.1421.

IWASZUK E., RUDIK G., DUIN L., MEDERAKE L., DAVIS M., NAUMANN S., WAGNER I. 2019. Addressing Climate Change in Cities – Catalogue of urban nature-based solutions. Ecologic Institute & the Sendzimir Foundation: Berlin, Cracow.

JARDEN K. M., JEFFERSON A. J., GRIESER J. 2015. Assessing the effects of catchment-scale urban green infrastructure retrofits on hydrograph characteristics. Hydrological Process 30, 10: 1536–1550, DOI:10.1002/hyp.10736.

JEFFERS S., GARNER B., HIDALGO D., DAOULARIS D., WARMERDAM O. 2022. Insights into green roof modeling using SWMM LID controls for detention-based designs. Journal of Water Management Modeling 30: C484. DOI:10.14796/JWMM.C484.

JIANG Y., YUAN Y., PIZA H. 2015. A Review of Applicability and Effectiveness of Low Impact Development/Green Infrastructure Practices in Arid/Semi-Arid United States. Environments, 2(2), 221-249; DOI:10.3390/environments2020221.

KASPRZYK M., SZPAKOWSKI W., POZNAŃSKA E., BOOGAARD F. C., BOBKOWSKA K., GAJEWSKA, M. 2022. Technical solutions and benefits of introducing rain gardens – Gdańsk case study. Science of The Total Environment 835, August 2022: 155487, DOI:10.1016/J.SCITOTENV.2022.155487.

KHAN, M. P., HUBACEK, K., BRUBAKER, K. L., ASCE, A. M., SUN, L., MOGLEN, G. E., ASCE, F. 2022. Stormwater Management Adaptation Pathways under Climate Change and Urbanization. Journal of Sustainable Water in the Built Environment 8, 4: 102290. DOI:10.1061/JSWBAY.0000992.

KORKOU M., TARIGAN A. K., HANSLIN, H. M. 2023. The multifunctionality concept in urban green infrastructure planning: A systematic literature review. Urban Forestry & Urban Greening 85: 127975. DOI:10.1016/j.ufug.2023.127975.

KRAVCHENKO M., WRZESIŃSKI G., PAWLUK K., LENDO-SIWICKA M., MARKIEWICZ A., TKACHENKO T., MILEIKOVSKYI V., ZHOVKVA O., SZYMANEK S., PIECHOWICZ K. 2024. Improving Urban Stormwater Management Using the Hydrological Model of Water Infiltration by Rain Gardens Considering the Water Column. Water 16, 16: 2339. DOI:10.3390/w16162339.

LEE J. G., NIETCH C. T., PANGULURI S. 2018. SWMM Modeling Methods for Simulating Green Infrastructure

at a Suburban Headwatershed: User's Guide (U.S. Environmental Protection Agency, Washington, DC, EPA/600/R-17/414).

LI C., LIU M., HU Y., GONG J., XU Y. 2015. Modeling the Quality and Quantity of Runoff in a Highly Urbanized Catchment Using Storm Water Management Model. Pol. J. Environ. Stud. 25, 4: 1573–1581. DOI: 10.15244/pjoes/60721.

LI C., LIU M., HU Y., SHI T., QU X., WALTER T. M. 2018. Effects of Urbanization on Direct Runoff Characteristics in Urban Functional Zones. Science of The Total Environment 643, 1 December 2018: 301–311. DOI:10.1016/j.scitotenv.2018.06.211.

LIN F., CHEN X., YAO, H. 2017. Evaluating the Use of Nash-Sutcliffe Efficiency Coefficient in Goodness-of-Fit Measures for Daily Runoff Simulation with SWAT. Journal of Hydrologic Engineering 22, 11. DOI:10.1061/(ASCE)HE.1943-5584.0001580.

LIU D., KWAN M.P., KAN Z., WANG, J. 2022. Toward a Healthy Urban Living Environment: Assessing 15-Minute Green-Blue Space Accessibility. Sustainability, 14, 24: 16914. DOI:10.3390/su142416914.

MAI Y., ZHANG M., CHEN W., CHEN X., HUANG G., LI D. 2019. Experimental study on the effects of LID measures on the control of rainfall runoff. Urban Water Journal 15, 9: 827–836. DOI:10.1080/1573062X.2018.1561912.

MAO Y., LI Y., BAI X., YANG X., HAN Y., FU X. 2024. Scenario-Based Green Infrastructure Installations for Building Urban Stormwater Resilience—A Case Study of Fengxi New City, China. Sustainability 16, 10: 3990. DOI:10.3390/su16103990.

MCCUTCHEON M., WRIDE, D. 2013. Shades of Green: Using SWMM LID Controls to Simulate Green Infrastructure. Journal Of Water Management Modeling 21: R246-15. DOI:DOI:10.14796/JWMM.R246-15.

MORIASI D. N., ARNOLD J. G., VAN LIEW M. W., BINGNER R. L., HARMEL R. D., VEITH T. L. 2007. Model Evaluation Guidelines for Systematic Quantification of Accuracy in Watershed Simulations. Transactions of the ASABE (American Society of Agricultural and Biological Engineers) 50, 3: 885–900. DOI:10.13031/2013.23153.

MULLER M. 2007. Adapting to climate change: water management for urban resilience. Environment and Urbanization 19, 1: 99–113. DOI:10.1177/0956247807076726.

MUSZYŃSKI K., GODYŃ I., PORĘBSKA A., RACOŃ-LEJA K. 2022. Koncepcja możliwości kształtowania bioretencji w zlewni Serafy z wykorzystaniem analiz przestrzennych naturalnych dróg spływu wód opadowych [The concept of the possibility of shaping bioretention in the Serafa catchment using spatial analyses of natural rainwater runoff routes]. Instal, 7, 8: 59–65. DOI:10.36119/15.2022.7-8.8.

NOWOGOŃSKI I., OGIOŁDA E., MUSIELAK M. 2019. Estimation of the Hydraulic Width of the Subcatchment Depending on the Degree of Detail of the Drainage System Model. Civil And Environmental Engineering Reports 29, 4: 128–140. DOI:10.2478/ceer-2019-0049.

NUR OKTALINOV FIKRI A., TJENDANI H. T., OETOMO W. 2022. Analysis of urban drainage system to avoid rain water overflow on the access road to Juanda Airport. The 8th International Conference of Euro Asia Civil Engineering Forum 1195, 1: 012045. DOI:10.1088/1755-1315/1195/1/012045.

PARNAS F. E. Å., ABDALLA E. M. H., MUTHANNA T. M. 2021. Evaluating three commonly used infiltration methods for permeable surfaces in urban areas using the SWMM and STORM. Hydrology Research 52, 1: 160–175. DOI:10.2166/nh.2021.048.

PN-EN 752:2017-06. 2017. Drain and sewer systems outside buildings - Sewerage system management.

PORĘBSKA A., MUSZYŃSKI K., GODYŃ I., RACOŃ-LEJA K. 2023. City and Water Risk: Accumulated Runoff Mapping Analysis as a Tool for Sustainable Land Use Planning. Land, 12, 7: 1345. DOI:10.3390/land12071345.

PRECIPITATION MODEL, Precipitation model for the City of Cracow. 2024. https://model-opadowy.wodociagi.krakow.pl/.

RAHMAN M. A., HARTMANN C., MOSER-REISCHL A., VON STRACHWITZ M. F., PAETH H., PRETZSCH H., PAULEIT S., RÖTZER T. 2020. Tree cooling effects and human thermal comfort under contrasting species and sites. Agricultural and Forest Meteorology 287, 15 June: 107947, DOI:10.1016/j.agrformet.2020.107947.

REZAEI A. R., ISMAIL Z., NIKSOKHAN M.H., DAYARIAN M. A., RAMLI A.H., SHIRAZI S.M. 2019. Quantity-Quality Model to Assess the Effects of Source Control Stormwater Management on Hydrology and Water Quality at the Catchment Scale. Water, 11, 7: 1415. DOI:10.3390/w11071415.

RESOLUTION No. XCVII/2493/18 of the Cracow City Council of 14 March 2018 on adopting a local spatial development plan for the "BRONOWICE - STELMACHÓW" area. 2018. Announced in the Official Gazette of the Małopolskie Voivodship of 23 March 2018, item 2238. https://www.bip.krakow.pl/?dok_id=96320.

ROESNER L. A., DICKINSON R. E. 1992. Storm Water Management Model User's Manual Version 4: Extra Addendum. Department of Environmental Engineering Sciences, University of Florida.

ROSSMAN L. A., HUBER W. C. 2016. Storm Water Management Model Reference Manual Volume III – Water Quality. National Risk Management Laboratory, Office of Research and Development, U.S. Environmental Protection Agency, Cincinnati, OH, USA (45268, EPA/600/R-16/093).

ROSSMAN L. A., SIMON M. A. 2022. Storm Water Management Model User's Manual Version 5.2. Center for Environmental Solutions and Emergency Response, Office of Research and Development, U.S. Environmental Protection Agency, Cincinnati, OH, USA. (45268,EPA-600/R-22/030).

ROY A. H., LEE R. K., MAYER A. L., SHUSTER W. D., BEAULIEU J. J., HOPTON M. E., MORRISON M. A., AMAND A. S. 2014. How Much Is Enough? Minimal Responses of Water Quality and Stream Biota to Partial Retrofit Stormwater

Management in a Suburban Neighborhood. Plos One 9, 1: e85011. DOI:10.1371/JOURNAL.PONE.0085011.

SHAMSI U. M., KORAN J. 2017. Continuous Calibration. Journal Of Water Management Modeling 25: C414. DOI:10.14796/JWMM.C414.

SINGH J., KNAPP H. V., DEM M. 2004. Hydrologic Modeling of the Iroquois River Watershed Using HSPF and SWAT. Illinois Department of Natural Resources and the Illinois State Geological Survey. Illinois State Water Survey Contract Report 2004-08.

SMITH J. S., WINSTON R. J., WITUSZYNSKI D. M., TIRPAK R. A., BOENING-ULMAN K. M., MARTIN, J. F. 2023. Effects of Watershed-Scale Green Infrastructure Retrofits on Urban Stormwater Quality: A Paired Watershed Study to Quantify Nutrient and Sediment Removal. Ecological Engineering 186, January 2023: 106835. DOI:10.1016/j.ecoleng.2022.106835.

SOFIJANIC A., HULLEY M., FILION Y. 2022. SWMM Stormwater Quality Model Developed to Assess the Performance of Best Management Practices: A Case Study of the Town of Jasper in Canada. Canadian Journal of Civil Engineering 50, 1: 24–33. DOI:10.1139/cjce-2021-0243.R1.

TACHE A.V., POPESCU O.C., PETRIȘOR A.I. 2023. Conceptual Model for Integrating the Green-Blue Infrastructure in Planning Using Geospatial Tools: Case Study of Bucharest, Romania Metropolitan Area. Land 12, 7: 1432. DOI:10.3390/land12071432.

TAREK M. H., KABIR S. M. I., ADIL H. 2017. Application of SWMM for analysis of flash floods in urban areas: A case study for Chaktai Khal watershed in Chittagong. Volume 6th International Conference on Water & Flood Management, Dhaka, Bangladesh (ICWFM-2017).

TITTERINGTON J., SQUIBBS G., DIGMAN C., ALLITT R., OSBORNE M., ECCLESTON P., WISDISH A. 2017. Code of Practice for the Hydraulic Modelling of Urban Drainage Systems 2017. The Chartered Institution of Water and Environmental Management (CIWEM), Version 01.

TIVERON T., GHOLAMREZA-KASHI S., JOKSIMOVIC D. 2018. A USEPA SWMM Integrated Tool for Determining the Suspended Solids Reduction Performance of Bioretention Cells. Journal Of Water Management Modeling. DOI:10.14796/JWMM.C443.

US ENVIRONMENTAL PROTECTION AGENCY. 2022. Storm Water Management Model User's Manual Version 5.2. United States Environmental Protection, Revised February 2022 (EPA/600/R-22/030).https://www.epa.gov/system/files/documents/2022-02/storm-water-management-model-users-manual-version-5.2.pdf.

WANG J., LIU J., WANG H., MEI C. 2020. Approaches to Multi-Objective Optimization and Assessment of Green Infrastructure and Their Multi-Functional Effectiveness: A Review. Water 12, 10: 2714, DOI:10.3390/w12102714.

WANG M., SUN Y., SWEETAPPLE C. 2017. Optimization of storage tank locations in an urban stormwater drainage system using a two-stage approach. Journal of Environmental Management 204, PART 1: 37–38. DOI:10.1016/j.jenvman.2017.08.024.

WANG M., ZHANG D. Q., SU J., DONG J. W., TAN S. K. 2018. Assessing hydrological effects and performance of low impact development practices based on future scenarios modeling. Journal of Cleaner Production 179, 1 April: 12–23. DOI:10.1016/j.jclepro.2018.01.096.

WANG S., HE Q., AI H., WANG Z., ZHANG Q. 2013. Pollutant Concentrations and Pollution Loads in Stormwater Runoff from Different Land Uses in Chongqing. Journal of Environmental Sciences 25, 3: 502–510, DOI:10.1016/S1001-0742(11)61032-2.

YIM S., AING C., MEN S., SOVANN, C. 2016. Applying PCSWMM for Stormwater Management in the Wat Phnom Sub Catchment, Phnom Penh, Cambodia. Journal of Geography, Environment and Earth Science International 5, 3: 1–11. ISSN: 2454-7352; DOI:10.9734/JGEESI/2016/23525.

ZHANG K., MAY CHUI T. F. 2019. A review on implementing infiltration-based green infrastructure in shallow groundwater environments: Challenges, approaches, and progress. Journal of Hydrology 579: 124089. DOI:10.1016/j.jhydrol.2019.124089.

ZHANG N., LUO Y., CHEN X., LI QI., JING Y., WANG X., FENG C. 2018. Understanding the Effects of Composition and Configuration of Land Covers on Surface Runoff in a Highly Urbanized Area. Ecological Engineering 125, December: 11–25. DOI:10.1016/J.ECOLENG.2018.10.008.